Title

Impulsivity Relates to Relative Preservation of Mesolimbic Connectivity in Patients with Parkinson Disease.

Authors

Sparks, Hiro
Riskin-Jones, Hannah
Price, Collin
et al.

Publication Date

2020

DOI

10.1016/j.nicl.2020.102259

Peer reviewed

NeuroImage: Clinical 27 (2020) 102259

Contents lists available at ScienceDirect

NeuroImage: Clinical

journal homepage: www.elsevier.com/locate/ynicl

Impulsivity Relates to Relative Preservation of Mesolimbic Connectivity in Patients with Parkinson Disease

Hiro Sparks[a,c], Hannah Riskin-Jones[a,c], Colin Price[b,c], Jasmine DiCesare[a,c], Ausaf Bari[a,c], Nadia Hashoush[a,c], Nader Pouratian[a,c,*]

[a] Department of Neurosurgery, 300 UCLA Stein Plaza, Suite 526
[b] Department of Psychiatry, 150 UCLA Medical Plaza Driveway
[c] David Geffen School of Medicine at UCLA (University of California, Los Angeles, CA, USA

ARTICLE INFO

Keywords:
Parkinson Disease
impulsivity
impulse control disorder
substantia nigra
diffusion tensor imaging

ABSTRACT

Introduction: The relationship between Parkinson Disease (PD) pathology, dopamine replacement therapy (DRT), and impulse control disorder (ICD) development is still incompletely understood. Given the sensorimotor-lateral substantia nigra (SN) selective degeneration associated with PD, we posit that a relative sparing of the limbic-medial SN in the context of DRT drives impulsive, reward-seeking behavior in PD patients with recent history of severe impulsivity.

Methods: Impulsive and control participants were selected from a consecutive list of PD patients receiving pre-operative deep brain stimulation (DBS) planning scans including 3T structural MRI and 64 direction diffusion tensor imaging (DTI). Using previously identified substantia nigra (SN) subsegment network connectivity profiles to develop classification targets, split-hemisphere target-based SN segmentation with probabilistic tractography was performed. The relative subsegment volumes and strength of connectivity between the SN and the limbic, associative, and motor network targets were compared.

Results: Our results show that there is greater probability of connectivity between the SN and limbic network targets relative to motor and associative network targets in PD patients with recent history of severe impulsivity as compared to PD patients without impulsivity ($P = 0.0075$). We did not observe relative volumetric subsegment differences across groups.

Conclusion: Firstly, our results suggest that fine-grained, atlas-derived classification targets may be used in PD to parcellate and classify functionally distinct subsegments of the SN, with the apparent preservation of previously reported topographical limbic-medial SN, associative-ventral SN, and sensorimotor-lateral SN orientation. We suggest that relative, as opposed to absolute, degeneration amongst SN-associated dopaminergic networks relates to the impulsivity phenotype in PD.

Introduction

Impulse control disorders (ICDs) are a heterogeneous group of disorders that involve pleasurable behaviors performed repetitively, excessively, and compulsively (Gatto & Aldinio, 2019; Jimenez-Urbieta et al., 2015; Maloney, Djamshidian, & O'Sullivan, 2017; Weintraub, David, Evans, Grant, & Stacy, 2015). The major manifestations of ICDs include pathological gambling (PG), hypersexuality (HS), compulsive buying/shopping (CB), and binge eating (BE) (Gatto & Aldinio, 2019). ICDs and related disorders have been included in the behavioral spectrum of non-motor symptoms in Parkinson disease (PD), and can often lead to financially, legally, and psychosocially devastating consequences with a disproportionate impact on patients' quality of life (Phu et al., 2014; Voon et al., 2009; Weintraub et al., 2015).

ICDs occur in 17.1% to 28.6% of PD patients on dopamine replacement therapy (DRT) (Antonini et al., 2017; Weintraub et al., 2010). Although DRT alone can influence reward-learning and increase impulsive behavior, the fact that ICDs only effect a subset of PD patients on equivalent DRT doses suggests the presence of intrinsic susceptibility factors underpinning the appearance of ICDs (Frank, Seeberger, & O'Reilly R, 2004; Tremblay, Hollerman, & Schultz, 1998; Voon et al., 2017). The relationship between PD pathology, dopamine replacement therapy (DRT), and ICDs is still incompletely understood (De Micco, Russo, Tedeschi, & Tessitore, 2018). Besides demographic, genetic, and

* Corresponding author. Department of Neurosurgery, 300 Stein Plaza, Suite 526, Los Angeles, California 90095, USA.
E-mail address: npouratian@mednet.ucla.edu (N. Pouratian).

https://doi.org/10.1016/j.nicl.2020.102259
Received 10 March 2020; Received in revised form 5 April 2020; Accepted 6 April 2020
Available online 22 April 2020

psychosocial variables, multiple imaging studies have identified morphologic and connectivity differences amongst PD patients with and without ICDs. Positron emission tomography (PET) studies have identified an association between the presence of ICDs in PD and a decrease in dopamine receptor availability in the ventral-limbic striatum, but not in the dorsal-motor striatum (Cilia et al., 2010; O'Sullivan et al., 2011; Payer et al., 2015; Steeves et al., 2009). These findings suggest an imbalance in dopamine signaling between sensorimotor-nigrostriatal and reward/learning-mesolimbic networks in PD patients with ICDs and have been interpreted according to either a hypo- or hyperdopaminergic theory. The hyperdopaminergic theory posits that decreased dopamine receptor availability reflects increased dopaminergic tone and as such DRT acts on the dopamine-depleted dorsal striatum and a relatively intact ventral striatum, reducing inhibitory signaling and leading to impairments in impulse control (De Micco et al., 2018; Gatto & Aldinio, 2019; Houeto, Magnard, Dalley, Belin, & Carnicella, 2016). Alternatively, these PET findings have been interpreted according to a hypodopaminergic theory in which decreased receptor availability stems from reduced dopaminergic neuron density and increased impulsivity may result from premorbid vulnerability in striatal connectivity to inhibitory regions (Hammes et al., 2019).

The loss of dopaminergic (DA) neurons in the substantia nigra pars compacta (SN) precipitates the cardinal motor symptoms of PD (Fearnley & Lees, 1991). Importantly, the progressive loss of DA neurons in PD begins in the ventrolateral portions of the SN with relative sparing of medial dopaminergic neurons at early stages (Duke, Moran, Pearce, & Graeber, 2007; Fearnley & Lees, 1991). This topographically-selective degeneration pattern is distinct from the dorsomedial SN-focused loss of dopaminergic neurons associated with normal aging (Fearnley & Lees, 1991). Recently, a magnetic resonance imaging (MRI) tractography-based parcellation scheme revealed a tripartite functional connectivity profile amongst SN sub-segments: the medial SN (mSN) most strongly connected to the ventral striatum and limbic networks; the lateral SN (lSN) most strongly connected to the dorsal striatum and sensorimotor networks; and the ventral SN (vSN) most strongly connected to the prefrontal cortex (PFC) and associative/executive networks (Zhang, Larcher, Misic, & Dagher, 2017). These results were consistent with the functional, topographic organization of the SN formerly observed in primate models using electrophysiologic and tracer stain experiments (Haber, 2014; Haber & Knutson, 2010; Matsumoto & Hikosaka, 2009).

Given the ventrolateral SN selective degeneration associated with PD, we posit that a relative sparing of the limbic-mSN in the context of DRT drives impulsive, reward-seeking behavior in PD patients with severe impulsivity. Using previously identified SN-subsegment network connectivity profiles to develop classification targets, we first performed target-based segmentation of the SN in PD patients with and without a history of severe impulsivity (Zhang et al., 2017). We then compared the relative strength of connectivity between the SN and the limbic, associative, and motor network targets, as measured by probabilistic tractography. Our hypothesis was that the connectivity between the mSN and limbic targets would show relative sparing compared to non-limbic-mSN networks in PD patients with a recent history of severe impulsivity.

Methodology

Subject Selection

Data for these analyses were retrospectively selected from consecutive PD patients who received 3T MRI with 64 direction diffusion tensor imaging (DTI) sequences as part of the UCLA deep brain stimulation program through January of 2013. All PD patients were diagnosed by Movement Disorder Society Criteria (Postuma et al., 2015). Of 163 patients in this group, 142 had complete, accessible imaging. These patients' medical records were reviewed for the presence of any ICDs or severe impulsivity. One author (HS) reviewed detailed pre-operative neuropsychological evaluation notes in addition to multiple years of neurological progress notes documenting adverse effects of medication. Patients were included if ICD was explicitly diagnosed in the EMR or if subjects were severely impulsive according to study criteria which were derived from modification of the Questionnaire for Impulsive-Compulsive Disorders in Parkinson's Disease (QUIP), Section 1, relating to compulsive gambling, buying, sexual, and eating behaviors (Weintraub et al., 2009). Our criteria required evidence that impulsivity symptoms interfered with financial, personal, family, and/or professional life, and that it could be reasonably inferred that any 1 of 5 QUIP criteria for gambling, sexual, and buying behaviors, or any 2 of 5 QUIP criteria for eating behaviors, was positive. Some example inferences include:

- QUIP A1 – Do you or others think you have an issue with ICD?
  - a example: dopaminergic medication regimen was modified or discontinued by patient or physician explicitly due to impulsive-compulsive behavior
  - b example from progress notes: "He reports dopamine agonist side effects, which is [sic] still present, including impulsivity when shopping, losing a lot of money gambling, and sexual compulsions including viewing a lot of pornography. He had attempted to taper himself off the dopamine agonist, but felt very unwell and off when he tried to do so"
- QUIP A2 – Do you think too much about the behaviors? No patient screened positive by this criterion.
- QUIP A3 – Do you have urges or desires for behaviors that you feel are excessive or distressing?
  - a example from progress notes: "He comes in today with his current girlfriend. He has been very embarrassed about the [sexual] ICD and feels that it has been effecting his relationship with his girlfriend."
- QUIP A4 – Do you have difficulty controlling ICD behaviors?
  - a example from progress notes: "[buying] to the point that his family has now removed all of his access to finances (e.g., daughter took away his credit cards)."
- QUIP A5 – Do you engage in activities (hiding, lying, borrowing, accumulating debt) to continue ICD behaviors?
  - a example from progress notes: "Of note, son at bedside has noted that he has been gambling without telling the family."

By these standards, 16 PD patients were determined to suffer from severe impulsivity, hereafter referred to as PD-impulsive group. Only those individuals with MRIs obtained within 2 years of symptomatic impulsivity period were included.

Following selection of PD-impulsive group, the same database records were retrospectively reviewed for control PD patient selection. Prior to imaging analysis, control subjects were consecutively selected to subjectively match the list of PD-impulsive subjects by age at MRI, age of PD onset, disease duration, Unified Parkinson's Disease Rating Scale (UPDRS-III)-off medications, years of education, and Levodopa Equivalent Daily Dose (LEDD). LEDD (as the sum of levodopa and dopamine agonist doses) was calculated according to the formula described by Tomlinson and colleagues (Tomlinson et al., 2010). Control subjects were excluded if there was a history of alcohol or other substance abuse.

We excluded any individuals who had a history of impulsivity that did not meet inclusion criteria, including mild/unimpairing impulsivity, punding, hobbyism, or dopamine dysregulation syndrome. All subjects screened negative for dementia, as part of pre-operative criteria for DBS. MRI images were screened by neuroradiologists and one author (HS) for focal changes including tumors, white matter FLAIR changes, or areas of encephalomalacia. All PD patients had been under stable dopaminergic therapy for at least two months at time of MRI.

We selected 16 PD patients without impulsivity to compose our PD-

control group. After thePD-control group was confirmed to match the PD-impulsive group for possible confounding clinical variables, no additional subjects were added to either group. All 32 patients underwent the following imaging analysis pipeline. One subject in the PD-control group failed cortical reconstruction, and was replaced by a well matched PD-control subject prior to group level analysis.

The study was approved by the institutional review board at UCLA.

Imaging

Each subject underwent 3T magnetic resonance imaging, including high resolution T1-weighted anatomical images (TR 11 ms, TE 2.81 ms, flip angle 20°, 0.9375 mm isotropic voxels, and 192 slices) and single shot spin echo planar imaging for diffusion tensor imaging (TR 9200 ms, TE 87 ms, 2 mm isotropic voxels, b value = 1000, and 64 directions).

Seed and Target Masks

FreeSurfer (version 5.3.0, http://surfer.nmr.mgh.harvard.edu/) was used for cortical surface reconstruction and volumetric segmentation (Dale, Fischl, & Sereno, 1999; Fischl, Sereno, & Dale, 1999). Cortical and subcortical labels were applied to subjects' native brains by using the Brainnetome Atlas Gaussian Classifier Surface (GCS) and Atlas (GCA) developed by Fan *et al* (available at http://atlas.brainnetome.org/download.html) in the Freesurfer pipeline (Fan et al., 2016). These labels were combined into conglomerate target masks representing the networks associated with SN connectivity. The groupings for these target masks were derived from an SN-parcellation study at the Montreal Neurological Institute that reported the relative probability of connectivity between functional SN subsegments and individual cortical and subcortical regions of interest (ROIs) in the Brainnetome atlas (Zhang *et al*, Supplemental Figure 5-1)(Zhang et al., 2017). In this study, Brainnetome ROIs were assigned to a respective network (i.e. limbic, associative, or motor) based on a winner take all approach. Lists of constituent ROIs for each network classification target mask are displayed in Table 1.

A mask of the SN was generated from a 7T MRI atlas of basal ganglia based on high-resolution MPRAGE and FLASH scans (Keuken and Forstmann, 2015. available at https://www.nitrc.org/projects/atag/), (Keuken & Forstmann, 2015). The entire region of the SN was extracted from the probabilistic atlas with a threshold of 33%, which is the same threshold that was used by Zhang *et al* (Zhang et al., 2017) to perform cluster segmentation of the SN. As our methods for segmentation rely on the classification targets derived from the Zhang *et al* analysis, alternative SN mask thresholds were not trialed.

The network-representative target masks and SN mask were registered to native patient DTI space using FSL. The MNI152 template and high resolution T1 images were first registered to native DTI space using a linear transformation (using mutual information as cost function, 6 degrees of freedom for DTI to T1 registration and 12 degrees of freedom for registration to MNI152). A nonlinear transformation was then applied to the MNI template and the appropriate transformation matrices were applied to each mask (Jenkinson, Bannister, Brady, & Smith, 2002). An example of appropriate transformation for single-subject SN and target masks is shown in Fig. 1.

Probabilistic Tractography

Probabilistic diffusion tractography was performed to measure

Table 1
Associative, limbic, and sensorimotor network representative classification target masks with constituent *Brainnetome atlas* regions of interest.

ventral-associative SN Target Masks,		medial-limbic SN Target Masks (Limbic)		lateral-sensorimotor SN Target Masks (Motor)	
Anatomical and modified Cyto-architectonic descriptions	Fan et al. nomenclature	Anatomical and modified Cyto-architectonic descriptions	Fan et al. nomenclature	Anatomical and modified Cyto-architectonic descriptions	Fan et al. nomenclature
A8m, medial area 8	SFG_c7_1	A35/36r, rostral area 35/36	PhG_c6_1	A6dl, dorsolateral area 6	SFG_c7_4
A8dl, dorsolateral area 8	SFG_c7_2	A35/36c, caudal area 35/36	PhG_c6_2	A6m, medial area 6	SFG_c7_5
A9l, lateral area 9	SFG_c7_3	TL, area TL (lateral PPHC)	PhG_c6_3	A6vl, ventrolateral area 6	MFG_c7_6
A9m, medial area 9	SFG_c7_6	A28/34, area 28/34 (EC, entorhinal cortex)	PhG_c6_4	Ahf, area 4 (head and face region	PrG_c6_1
A10m, medial area 10	SFG_c7_7	A28/34, area 28/34 (EC, entorhinal cortex)	PhG_c6_5	A6cdl, caudal dorsolateral area 6	PrG_c6_2
A9/46d, dorsal area 9/46	MFG_c7_1	TH, area TH (medial PPHC)	PhG_c6_6	A4tul, area 4 (upper limb region)	PrG_c6_3
A46, area 46	MFG_c7_3	rHipp, rostral hippocampus	Hipp_c2_1	A4t, area 4 (trunk region)	PrG_c6_4
A9/46v, ventral area 9/46	MFG_c7_4	cHipp, caudal hippocampus	Hipp_c2_2	A4tl, area 4 (tongue and larynx region)	PrG_c6_5
A8vl, ventrolateral area 8	MFG_c7_5	mAmyg, medial amygdala	Amyg_c2_1	A6cvl, caudal ventrolateral area 6	PrG_c6_6
A10l, lateral area 10	MFG_c7_7	lAmyg, lateral amygdala	Amyg_c2_2	A1/2/3ulhf, area 1/2/3(upper limb, head and face region)	PoG_c4_1
A44d, dorsal area 44	IFG_c6_1	vCa, ventral caudate	BG_c6_1	A1/2/3tonIa, area 1/2/3(tongue and larynx region)	PoG_c4_2
IFS, inferior frontal sulcus	IFG_C6_2	NAC, nucleus accumbens	BG_c6_3	A2, area 2	PoG_c4_3
A45c, caudal area 45	IFG_C6_3	vmPu, ventromedial putamen	BG_c6_4	A1/2/3tru, area1/2/3(trunk region)	PoG_c4_4
A45r, rostral area 45	IFG_C6_4	dlPu, dorsolateral putamen	BG_c6_6	A39c, caudal area 39	IPL_c6_1
A44op, opercular area 44	IFG_C6_5			A39rd, rostrodorsal area 39	IPL_c6_2
A44v, ventral area 44	IFG_C6_6			A40rd, rostrodorsal area 40	IPL_c6_3
GP, globus pallidus	BG_c6_2			A40c, caudal area	IPL_c6_4
				A39rv, rostroventral area	IPL_c6_5
				A40rv, rostroventral area	IPL_c6_6
				A7r, rostral area 7	SPL_c5_1
				A7c, caudal area 7	SPL_c5_2
				A5l, lateral area 5	SPL_c5_3
				A7pc, postcentral area 7	SPL_c5_4
				A7ip, intraparietal area 7	SPL_c5_5
				dCa, dorsal caudate	BG_c6_5

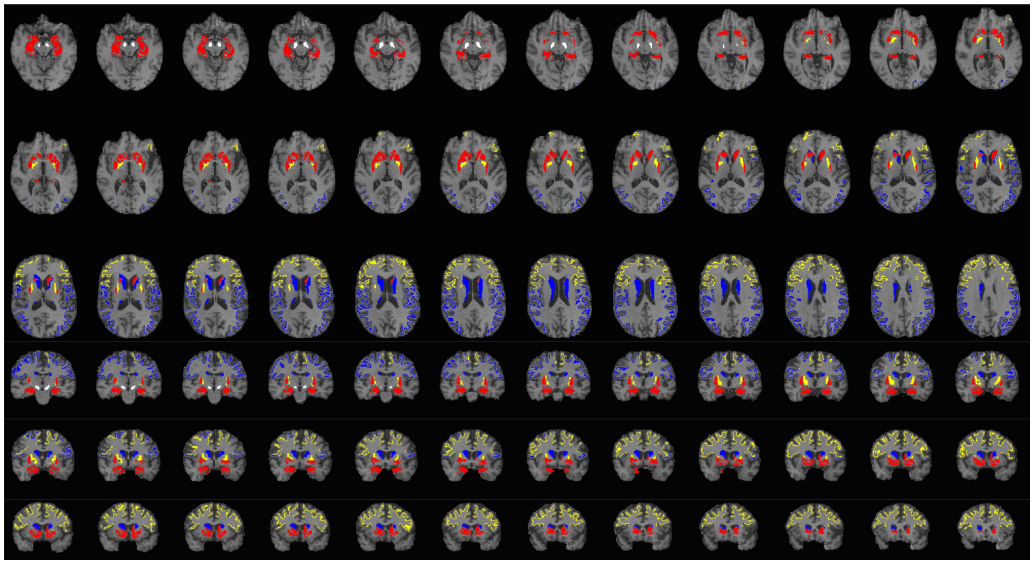

Figure 1. Single subject substantia nigra seed, white. Three network representative classification target masks include: limbic, red; associative, blue; and sensorimotor, yellow.

structural connectivity between the SN and the three network-representative target masks using the FMRIB's Diffusion toolbox (FDT). Eddy current correction was used to apply affine registrations to each volume in the diffusion dataset to register it with the initial reference B0 volume prior to performing tractography. Skull stripping was performed using the FMRIB brain extraction tool (BET), (Smith, 2002). A multi-fiber diffusion model in FDT was fitted to the data. This model uses Bayesian techniques to estimate a probability distribution function (PDF) on the principal fiber direction at each voxel, accounting for the possibility of crossing fibers within each voxel (Behrens, Berg, Jbabdi, Rushworth, & Woolrich, 2007). Two fibers were modeled per voxel, a multiplicative factor (i.e., weight) of 1 for the prior on the additional modeled fibers, and 1000 iterations before sampling (Behrens et al., 2007). Using these PDFs and PROBTRACKX, we could then determine the probability of connectivity between SN and each classification target mask. Analysis was performed on split hemispheres. From each voxel in the SN, 5000 streamlines were generated; the FSL default 0.2 curvature threshold was used, a loop check termination was used, and the target masks were used as classification masks. Probabilistic tractography methods were previously described by Tsolaki *et al*(Tsolaki, Downes, Speier, Elias, & Pouratian, 2018).

Threshold Determination

In order to prevent excessive censoring of single subjects with low probability of connectivity and to ensure that all subjects were contributing to grouped statistics, the probability of connectivity between each subject's seed-voxel and network-representative target mask was normalized by subject hemisphere-specific maximum probability of connectivity (e.g. if the range of voxel-wise probabilities of SN to limbic target connectivity was 0.01– 0.6, then all probabilities were divided by 0.6 and reported as a percent of maximum probability of connectivity) (Tsolaki et al., 2018). For each patient, we used the voxel-wise percent of maximum probability of connectivity to compute voxel-wise percentiles within each hemisphere. These percentiles were plotted against the percent of maximum connectivity to limbic targets in order to visualize potential thresholds (Fig. 2A). There appeared to be two populations of voxels within each subject specific SN mask, where on average, roughly 50% of all voxels within a SN mask demonstrate $<25\%$ of the maximum probability connectivity to limbic targets, whereas the remaining 50% demonstrated a relatively broad range of 25%-100% of maximal connectivity. Thus, an arbitrary threshold of 25% of maximal connectivity was applied to each respective probabilistic seed mask. Visual inspection of similar distributions for associative-vSN and motor-lSN connectivity analyses did not reveal an intuitive point for thresholding, thus the same threshold of 25% of maximal connectivity to respective targets were applied. These distributions are plotted in Fig. 2B and 2C.

Statistical Analysis

In order to test the hypothesis that relative SN subsegment degeneration relates to impulsivity in PD, two planned comparisons were initially made. The ratio of connectivity probabilities between of limbic-mSN relative to mean motor-lSN and associative-vSN were compared across groups. The limbic-mSN subsegment volumes relative to mean motor-lSN and associative-vSN volumes were compared across groups.

Following a priori testing, three post-hoc analyses were performed: comparison of absolute limbic-mSN connectivity probability across groups; comparison of limbic-mSN relative to motor-lSN connectivity; and comparison of limbic-mSN relative to associative-vSN connectivity.

To explore connectivity and volume comparisons between the PD-impulsive and PD-control groups, t-tests were performed with hemispheric data. The threshold value for the significance of group differences was $p<0.05$ for two planned analyses ($p<0.025$ after Bonferonni correction) and $p<0.01$ for three additional post-hoc analyses. To further account for the inter-dependence of within subject measurements and to control for LEDD, a multivariate linear mixed effect regression model was created to relate connectivity to impulsivity, modeling LEDD as fixed effects and subject as random effects.

To confirm the robustness of significant results over multiple thresholds, sensitivity analysis was performed by taking the area under the curve of receiver operator characteristic curves at multiple thresholds (shown as vertical lines in Fig. 2A). The use of confirmatory models or different connectivity thresholds for robustness testing were not considered unique comparisons requiring correction, as the tested hypotheses and data were unchanged.

All statistical tests were performed with R (RStudio Team (2015). Integrated Development for R. RStudio, Inc., Boston, MA URL http://www.rstudio.com/).

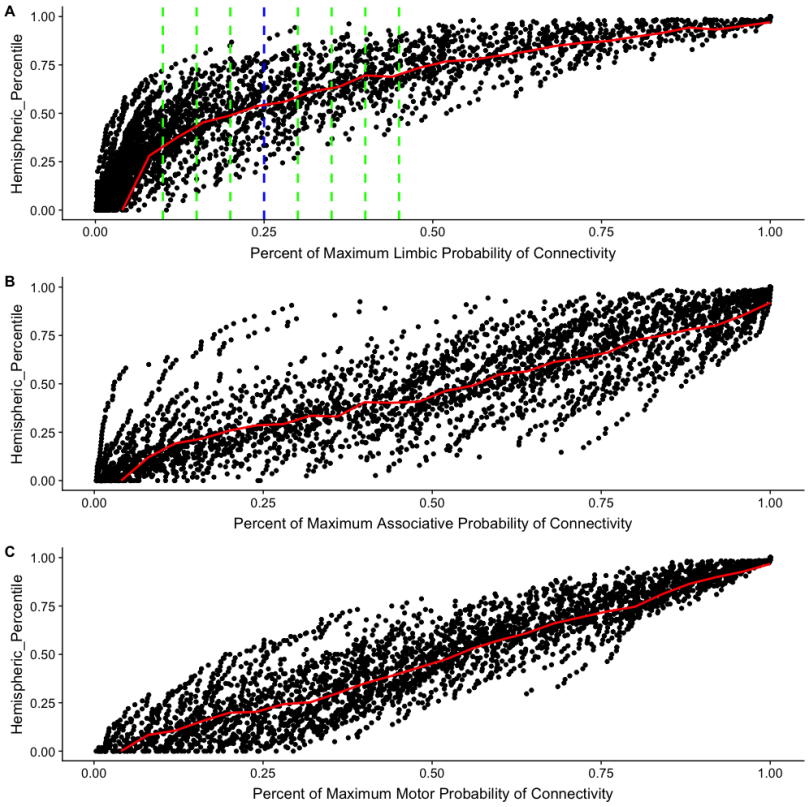

Figure 2. Scatter plot of connectivity percentile amongst voxels in a single subject SN versus percent of maximum connectivity for each SN voxel to **A)** limbic, **B)** associative, **C)** sensorimotor targets. Red solid line shows average percentile at each percent of maximum value across all subjects. Blue dashed line shows the initial 25% of maximum probability of connectivity threshold applied to all SN masks. Green dashed line shows alternative thresholds selected for robustness testing.

Results

Demographics

The PD-impulsive group (n = 16) and PD-control group (n = 16) did not significantly differ with respect to demographic variables including age, sex, UPDRS-III, PD symptom duration, LEDD, and years of education (Table 2).

Classification Based SN Segmentation

Tomographic maps identifying the regions within the SN with the highest probability of connectivity to limbic, associative, and sensorimotor masks were created. A probabilistic map for a single subject is demonstrated in Fig. 3A-C. Individual seed voxel-wise probability of target connectivity was averaged across individuals within each group.

Table 2
Baseline subject characteristics.

	PD-Impulsive, n = 16	PD-Control, n = 16	Test	
Average age at MRI, years, mean (SD)	61.5 (7.0)	64.0 (7.9)	T-Test	p = 0.34
M/F	13/3	13/3	Chi-squared	P = 0.65
3T, 64 dir DTI	16	16		-
Average UPDRS III Off, mean (SD)	36.0 (16.8), n = 15	43.1 (19.6), n = 14	T-Test	p = 0.30
PD Symptom Duration at MRI, months, mean (SD)	109.5 (33.1)	112.6 (46.2)	T-Test	0.83
LEDD, mg, mean (SD)	1398.6 (414.1)	1164.6 (695.7)	T-Test	p = 0.26
Education				
>16 years	5	4	Chi-squared	p = 0.77
12-16 years	6	4	Chi-squared	p = 0.51
8-12 years	2	2	Chi-squared	p = 0.94
<8 years	1	1	Chi-squared	p = 0.96
Unavailable	2	5	Chi-squared	p = 0.20
ICD Duration, months, mean (SD)	24.1 (35.0)	-	-	-
Time from last reported ICD to MRI, months, mean (SD)	7.7 (7.0)	-	-	-
ICD Selection Method				
Severe Impulsivity Criteria	7 (43.8%)	-	-	-
Charted Diagnosis	9 (56.2%)	-	-	-
Buying	5	-	-	-
Eating	1	-	-	-
Gambling	4	-	-	-
Hypersexuality	4	-	-	-
Hypersexuality + eating	1	-	-	-
Buying + gambling	1	-	-	-

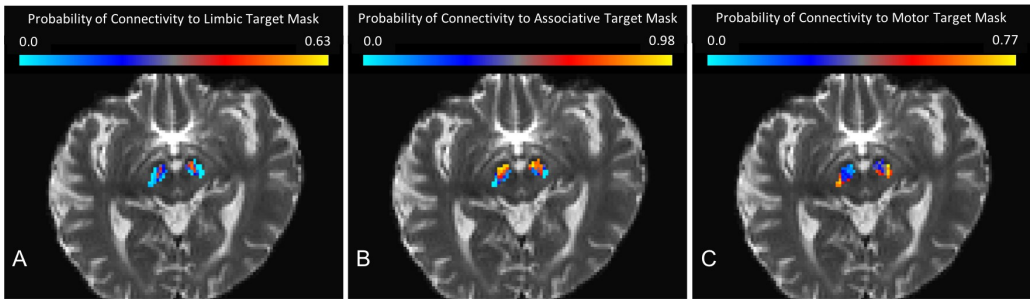

Figure 3. Single subject tomographic probability maps representing probability of connectivity within each voxel of the SN and **A)** limbic target **B)** associative/executive target **C)** sensorimotor target.

For visualization purposes, these average maps were binarized at 25%, 50%, and 75%, and projected onto a 3-dimensional Standard MNI 152 brain (Fig. 4). SN subregions are consistent with the expected results from prior work: voxels in the dorsomedial SN demonstrated the highest probability of connectivity to limbic targets; dorsolateral SN demonstrated the highest probability of connectivity to sensorimotor targets; and ventral SN demonstrated the highest connectivity to associative targets (Zhang et al., 2017). We evaluated different probability thresholds to ensure that selection of threshold did not bias or affect results. Different probability thresholds do not change the organizational pattern, but only enlarge or shrink the coverage of overlapping functional subsegments.

In regards to volume, there were no differences between groups when comparing mSN to the lSN and the vSN (Fig. 5B, Table 3).

After thresholding at 25% of maximum probability of connectivity, relative connectivity strength was found to be significantly greater in PD-impulsive group when comparing limbic-mSN to mean probabilities of sensorimotor-lSN and associative-vSN connectivity $P<0.0075$ (Fig. 5A). This result was robust across multiple tested thresholds (Table 3). When tested in a multivariate mixed regression model which controlled for both LEDD and within subject measures, impulsivity correlated with greater relative connectivity across multiple thresholds (Table 3). An example of summary statistics for this model at 25% percent of maximum probability of connectivity is shown in Table 4. Interestingly, a negative interaction term for impulsivity and LEDD trended toward significance. The plot of connectivity as a function of the interaction between impulsivity and LEDD is shown in Fig. 6.

Post-hoc analyses revealed a trend toward absolute limbic-mSN connectivity being greater in the PD-impulsive relative to PD-control groups, (Fig. 5C, Table 5). Additionally, there was a trend toward greater limbic-mSN connectivity relative to individual motor-lSN or associative-vSN subsegments, depending on selected thresholds (Fig. 5D, 5E and Table 5). All post-hoc trends were not significant after correction for multiple comparisons.

Discussion

Relative Probability of Connectivity

PD patients with a recent history of severe impulsivity demonstrate significantly greater probability of connectivity between the SN and limbic network targets relative to motor and prefrontal network compared to PD patients without impulsivity. These results contribute to a growing body of evidence that differential degeneration across SN-associated dopaminergic networks determines the impulsivity phenotype (De Micco et al., 2018; Joutsa et al., 2012; H. B. Yoo et al., 2015). This also fits with the model that while DRT partially restores the normal functioning within the nigrostriatal network (improving motor symptoms), the dopaminergic treatment may overload the mesolimbic network, potentially triggering affective disturbances and impulsivity (Cools, de Pauw, & Vanderheyden, 2011; De Micco et al., 2018; Wise, 2009).

These findings are consistent with prior reports of PD patients with ICDs demonstrating marked decreases in ventrostriatal and unchanged dorsostriatal DA-receptor expression at baseline (Payer et al., 2015). Other studies have confirmed increased ventrostriatal - but not

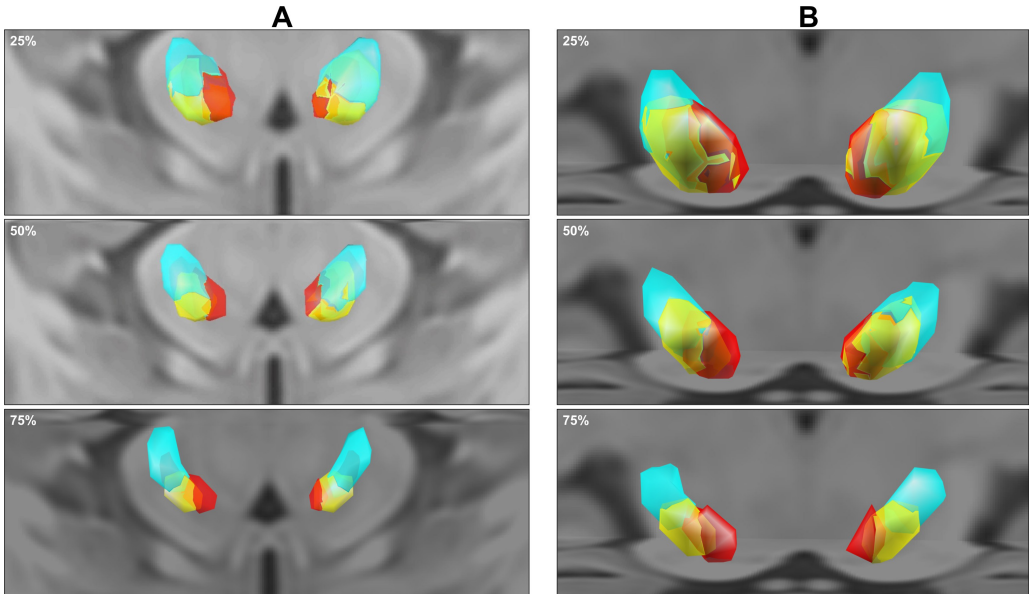

Figure 4. A) Superior-inferior **B)** anterior-posterior view of group averaged probabilistic SN connectivity maps thresholded and binarized at 25%, 50%, and 75% probability of connectivity to respective targets and projected in front of a 3-dimensional Standard MNI 152 brain. Voxels with supra-threshold connectivity to limbic, associative, sensorimotor targets are displayed as red, yellow, blue, respectively. PD-impulsive group is anatomical left, n = 32. PD-control group is anatomical right, n = 32.

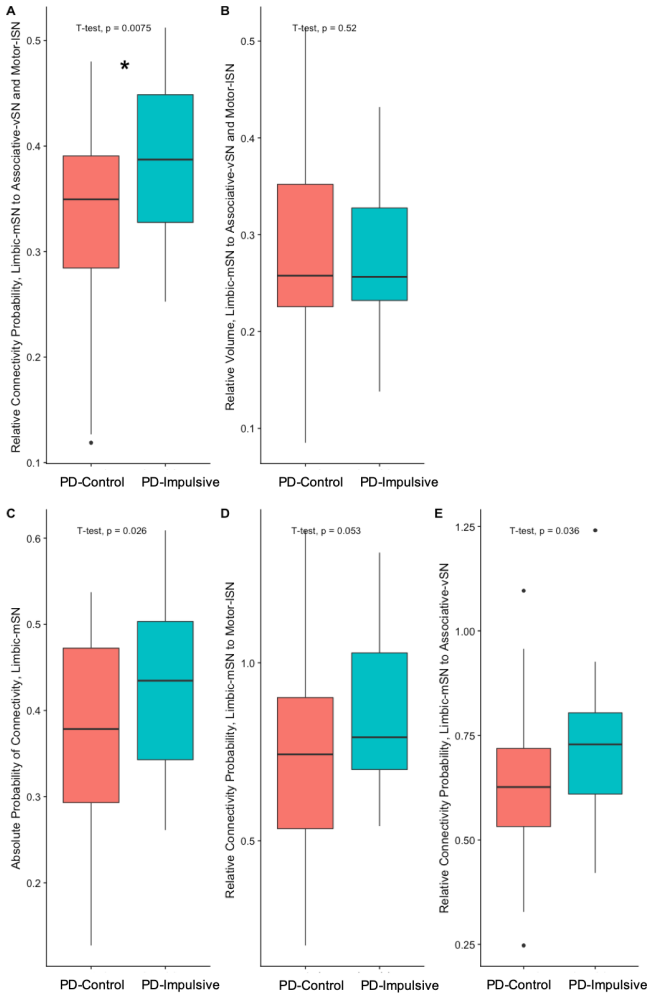

Figure 5. Thresholded at 25% of hemisphere-target specific maximum probability of connectivity **A)** ratio of limbic-mSN relative to associative-vSN and motor-lSN connectivity **B)** ratio of mSN relative to vSN and lSN voxel count **C)** limbic-mSN probability of connectivity **D)** ratio of limbic-mSN relative to motor-lSN probability of connectivity **E)** ratio of limbic-mSN relative to associative-vSN probability of connectivity. Asterisk denotes statistical significance after correction for multiple comparisons.

Table 4
Results of multivariate linear mixed effect regression taken at 25% of maximum connectivity threshold. Relative connectivity as a function of impulsivity and LEDD, with subject as a random effect.

Relative Connectivity Probability, Limbic-mSN to Asscoiative-vSN and Motor-lSN				
Variables	*Coefficient*	*df*	*t value*	*p*
LEDD	0.29	28	1.34	0.19
PD-Impulsive vs PD-Control	0.20	28	2.71	0.011*
LEDD: PD-Impulsive vs PD-Control	-1.1e-4	28	-2.1	0.048*
Random Effects				
σ	0.057			
N_{ID}	32			
Observations	64			
Marginal R^2 / Conditional R^2	0.187 / 0.583			

dorsostriatal - DA release in response to reward cues amongst PD patients with ICDs (O'Sullivan et al., 2011; Steeves et al., 2009). Furthermore, experimental PD models have shown an increase in DA levels in the nucleus accumbens/ventral striatum following selective nigrostriatal (motor) DA denervation (Houeto et al., 2016; van Oosten, Verheij, & Cools, 2005). These findings, of a diminished ventrostriatal DA receptor level and an increase in mesolimbic DA tone, are both hallmark features of a high impulsivity trait in humans and rats, and may explain the increased propensity to develop impulsive behaviors in PD (Besson et al., 2013; Buckholtz et al., 2010; Dalley et al., 2007; Diergaarde et al., 2008). Multiple additional multimodal neuroimaging studies have corroborated the relative preservation of limbic networks and related nodes amongst impulsive rather than non-impulsive PD patients—including mPFC, OFC, amygdala, and habenula—although some of these reported changes have been inconsistent (Cerasa et al., 2014; Claassen et al., 2017; Loane et al., 2015; Markovic et al., 2017; Tessitore et al., 2017; Tessitore et al., 2016). The hyperdopaminergic hypothesis is further supported by the mixed linear regression model which suggested a trend toward SN connectivity as a function of the interaction between impulsivity and LEDD. Specifically, at low LEDD the impulsivity phenotype is strongly associated with larger relative mesolimbic connectivity. This suggests that individuals with impulsivity at lower LEDD demonstrte mesolimbic intactness and sensitivity to dopaminergic medication. Whereas at high LEDD, relative connectivity of the mesolimbic network does not select for the impulsivity. To that end, we predict that there is some LEDD at which most PD patients will display some level of impulsivity regardless of

Table 3
Comparison of limbic connectivity and volume relative to non-limbic (associative and motor) segments of the substantia nigra (SN). Results are shown across multiple thresholds. Mixed Regression Model column reports p-value associated with correlation between relative connectivity and impulsivity while controlling for LEDD and interhemispheric measurement dependence within subjects.

	Relative Volume (Limbic-mSN versus Associative-vSN and Motor-lSN)			Relative Connectivity (Limbic-mSN versus Associative-vSN and Motor-lSN)				
Percent of Maximum Connectivity Threshold	Impulsive, mean +/- SD	Control, mean+/-SD	P Val	Impulsive, mean +/- SD	Control, mean+/-SD	P Val	AUC	Mixed Regression Model, P Val
10	0.337+/-0.0653	0.355+/-0.0906	0.370	0.334+/-0.0576	0.287+/-0.0921	0.017*	0.655	0.044
15	0.306+/-0.0607	0.324+/-0.101	0.404	0.358+/-0.064	0.306+/-0.09	0.010*	0.661	0.034
20	0.29+/-0.0665	0.305+/-0.1	0.482	0.374+/-0.0728	0.318+/-0.0929	0.009*	0.664	0.015*
25	0.272+/-0.0683	0.286+/-0.106	0.522	0.387+/-0.0699	0.329+/-0.0951	0.008*	0.665	0.011*
30	0.262+/-0.0702	0.265+/-0.105	0.916	0.393+/-0.0703	0.341+/-0.0996	0.019*	0.644	0.011*
35	0.248+/-0.071	0.257+/-0.111	0.689	0.401+/-0.0693	0.339+/-0.116	0.013*	0.656	0.016*
40	0.238+/-0.0737	0.252+/-0.12	0.575	0.406+/-0.0699	0.342+/-0.115	0.009*	0.671	0.013*
45	0.228+/-0.079	0.234+/-0.124	0.805	0.414+/-0.0712	0.354+/-0.122	0.020*	0.655	0.019*
50	0.224+/-0.0882	0.228+/-0.122	0.868	0.417+/-0.0694	0.355+/-0.12	0.015*	0.663	0.023*

* denotes statistical significance after correction for multiple comparisons; Green highlighter denotes statistical trend prior to correction for multiple comparisons; AUC, area under the curve for the receiver operator characteristic curve created by a logistic model; lSN, lateral SN; mSN, medial SN; vSN, ventral SN

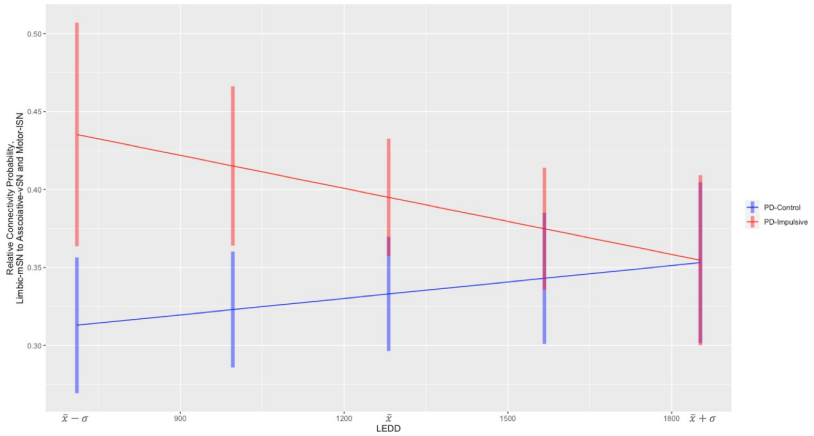

Figure 6. Plot of mixed effect linear regression model at 25% of maximum probability of connectivity: relative connectivity as a function of LEDD and impulsivity. Vertical bars indicated 95% confidence intervals. The model is plotted over of +/-1 standard deviation of the whole cohort LEDD mean.

Table 5
Post-hoc comparisons of absolute limbic connectivity, limbic-medial SN connectivity relative to motor-lateral SN, and limbic-medial SN connectivity relative to associative-ventral SN. Results are shown across multiple thresholds.

	Absolute Probability (Limbic-mSN Connectivity)			**Relative Connectivity (Limbic-mSN versus Motor-lSN)**			**Relative Connectivity (Limbic-mSN versus Associative-vSN)**		
Percent of Maximum Connectivity Threshold	Impulsive, mean +/- SD	Control, mean+/-SD	P Val Abs	Impulsive, mean +/- SD	Control, mean+/-SD	P Val	Impulsive, mean +/- SD	Control, mean+/-SD	P Val
10	0.332+/-0.0812	0.279+/-0.111	0.034	0.754+/-0.188	0.667+/-0.301	0.171	0.623+/-0.129	0.547+/-0.176	0.052
15	0.367+/-0.0886	0.311+/-0.11	0.029	0.814+/-0.214	0.707+/-0.293	0.099	0.662+/-0.139	0.582+/-0.174	0.046
20	0.398+/-0.099	0.338+/-0.115	0.028	0.843+/-0.23	0.727+/-0.293	0.084	0.695+/-0.158	0.602+/-0.183	0.033
25	0.427+/-0.101	0.363+/-0.119	0.026	0.867+/-0.225	0.739+/-0.29	0.054	0.722+/-0.154	0.628+/-0.194	0.036
30	0.448+/-0.102	0.391+/-0.124	0.048	0.878+/-0.224	0.758+/-0.281	0.063	0.734+/-0.15	0.65+/-0.204	0.068
35	0.472+/-0.102	0.405+/-0.146	0.037	0.89+/-0.218	0.745+/-0.295	0.029	0.753+/-0.148	0.65+/-0.236	0.041
40	0.494+/-0.103	0.424+/-0.149	0.033	0.891+/-0.207	0.736+/-0.273	0.014	0.769+/-0.15	0.661+/-0.238	0.036
45	0.52+/-0.104	0.452+/-0.161	0.050	0.899+/-0.205	0.756+/-0.279	0.022	0.787+/-0.152	0.685+/-0.253	0.058
50	0.542+/-0.103	0.469+/-0.167	0.041	0.897+/-0.191	0.759+/-0.279	0.025	0.798+/-0.154	0.686+/-0.244	0.032

Green highlighter denotes statistical trend prior to correction for multiple comparisons; lSN, lateral SN; mSN, medial SN; vSN, ventral SN

relative SN connectivity. Within the tested group, the selective appearance of impulsivity at higher ranges of LEDD may due to some other network dysfunction. For example, a series of studies have also identified a "frontal-striatal dysconnectivity syndrome" in which reductions in connectivity between striatum and frontal regions, most prominently anterior cingulate cortex (an inhibitory region connected to the mesolimbic network) are associated with impulsivity in PD (Cilia et al., 2011; Hammes et al., 2019; Premi et al., 2016). It may be that limbic connectivity changes are non-uniform across the network and additional multimodal studies at a nodal level are warranted to clarify these complexities in the context of ICDs.

One potential mechanism for frontal-striatal dysfunction may result from tonic overloading of networks with D2/D3 receptor agonists (e.g., pramipexole and ropinirole). This is thought to suppress reward-related learning by attenuating the effects of negative feedback on phasic dopamine release, thereby encouraging compulsive, perseverative behavior through a direct D1 receptor pathway. That is, excessive striatal D2/D3 agonism diminishes inhibitory control by PFC and other nodes in the executive network (Goto & Grace, 2008; Rokosik & Napier, 2012). Of interest, we found a trend toward degeneration of associative-vSN connectivity as compared to limbic-mSN connectivity. Relative degeneration of associative network nodes has also been implicated in the development of impulsivity in multiple prior imaging studies (Biundo et al., 2015; Markovic et al., 2017; Ruitenberg et al., 2018; Tessitore et al., 2017; H. S. Yoo et al., 2015).

An alternate theory to the "overload" hypothesis suggests that impulsivity in PD is associated with decreased dopamine synthesis and storage in the ventral striatum paired with constitutionally decreased or degenerated fronto-striatal connectivity. In this model, metabolic imaging studies finding decreased DAT or D2 receptor availability (e.g. Cilia 2011, Steeves 2009) are interpreted as reflecting decreased dopaminergic neuron density. This hypodopaminergic theory is supported by Hammes *et al* 2019, a study which found decreased F-DOPA signal in the nucleus accumbens of PD patients with impulsivity, similar to non-PD addictive phenotypes (Hammes et al., 2019; Majuri & Joutsa, 2019). Functional imaging studies have also found decreased activity in the ventral striatum at rest and in response to risk taking tasks(Rao et al., 2010; Voon et al., 2011). In this context, decreased dopamine signaling paired with fronto-striatal dysconnectivity (as discussed above) is thought to underly the impulsivity phenotype (Hammes 2019, Cilia 2011)(Cilia et al., 2011; Hammes et al., 2019). Increased connectivity of the SN (as shown in this report) to a dysfunctional limbic network may exacerbate increased impulsivity among PD patients with these traits. However, our study was not designed to definitively differentiate between the hypo- and hyper-dopaminergic models. In particular, connectivity was not analyzed between multiple nodes in each network which might elucidate structural connectivity changes underlying a fronto-striatal dysconnectivity syndrome, but rather between SN and composite target masks intended to capture overall network status.

Rather than serving as an etiology of impulsivity, it is also possible that the differential pattern of SN connectivity in the impulsive PD group may have been caused by the development of impulsive behavior. That is, frequent execution of uncontrolled behaviors in PD patients with increased impulsivity may result in a modification of tissue

integrity, contributing to greater neurotransmission between regions. These changes may be represented on imaging by stronger fractional anisotropy or directionality of neuronal fibers. The pathological tendency to repeat impulsive behaviors not only creates signal overflow but may theoretically remodel related structures and white matter pathways (H. B. Yoo et al., 2015). Based on the current analyses, one cannot determine whether these findings reflect the effect of chronic dopaminergic treatment or represent a neural pattern predisposing to impulsivity (Voon et al., 2017).

Relative Volumes

Our results demonstrate that fine-grained, atlas-derived classification targets may be used in PD to parcellate and classify functionally distinct subsegments of the SN, with the apparent preservation of previously reported topographical limbic-mSN, prefrontal-vSN, and sensorimotor-lSN orientation (Zhang et al., 2017). In the context of a relatively preserved limbic-mSN dopaminergic network—and with knowledge that PD-associated progressive neuronal degeneration initially occurs in ventrolateral rather than medial SN—we expected to observe relative volumetric subsegment differences across groups (Fearnley & Lees, 1991). Contrary to our hypothesis, these differences were not observed. Nonetheless, this is the first report which uses DTI to assert the in-vivo functional topographical organization of the SN in PD. Moreover, despite the absence of volumetric changes, we provide evidence for the relative segmental degeneration of ventrolateral SN areas as assessed by probabilistic connectivity differences.

Limitations

The classification target masks were determined based on a previous study's subsegment connectivity profiles using a “winner-takes-all” approach which assigns each brain area to only one network (Zhang et al., 2017). In reality, there are overlapping functional regions within the SN and most target masks connect to multiple SN subdivisions to some degree. Furthermore, previous parcellations did not account for white matter tracts that travel within the SN before leaving the seed area. Our finding that the limbic mask shows the strongest connection to the mSN could be partially explained by the fact that a majority of fibers from the lSN travel medially, before turning dorsally toward the striatum. Thus, using tractography to interpret the relative degradation of particular subdivisions of the SN has intrinsic limitations. Nonetheless, the present research represents an exploratory study, with any significant results representing intriguing targets for further work rather than a definitive statement on SN connectivity in PD.

Additionally, our hypothesis is partially predicated upon the dynamic nature of network degeneration in PD; that is, there may be a time-dependent relative degeneration of motor-lateral and associative-ventral SN compared to the limbic-medial SN. Thus, the cross-sectional nature of our clinical data is an inherent limitation to this study. As such, we assume some time window following ventrolateral degeneration – but prior to medial degeneration –where impulsive behavior is most correlated to structural connectivity measures in SN-associated networks. This hypothesis has never been previously investigated, as it would require prospective testing with serial DTI scans preceding and following impulsive periods. To ensure that we were indeed capturing structural connectivity measurements relating to impulsivity, we excluded subjects with symptom resolution greater than 2 years prior to scanning. Given that our data was sourced from pre-operative DBS planning scans, most patients were necessarily mildly impulsive or asymptomatic at the time of surgical planning, due to surgeon preference. Thus, there remains a possibility that the structural connectivity findings reported in this study were unrelated to the patient's history of impulsivity or were stochastic.

This study is also limited by the available clinical data from our institution. The sample size of 16 per group introduces both the possibility that these results would not be generalizable to a larger population and increases the likelihood of type 2 error. Additionally, the cohort included in this report are patients seen for surgical planning for DBS, and may not be representative of a general PD sample. Finally, for a select subset of patients without a formal explicit diagnosis of ICD, patient selection was performed using QUIP criteria retrospectively administered using provider progress notes. Although the authors felt that this method of patient selection was well-defined, this is not the intended method for which the QUIP was developed. When administered directly to the patient, the QUIP, section 1, has $>89\%$ specificity for true ICD (Weintraub et al., 2009). Without additional data it is impossible to ascertain the specificity of the QUIP when administered in this retrospective manner, and therefore it cannot be determined if patients had true ICDs, although some pathological degree of impulsivity at the time of the written progress note is evident. Again, this study was intended to explore differences between impulsive and non-impulsive PD patients, rather than serve as a method for diagnostic validation. Along these lines, punding, hobbyism, and dopamine dysregulation syndrome were not included, as retrospectively assessing pathological limits was challenging and inconsistent. Indeed, the increased drive or motivation to perform certain behaviors may be beneficial rather than harmful (Gatto & Aldinio, 2019; Weintraub et al., 2015).

Conclusions

We use network-representative target masks to parcellate and classify functionally distinct subsegments of the SN in PD patients, with the apparent preservation of previously reported topographical limbic-mSN, prefrontal-vSN, and sensorimotor-lSN anatomic subdivisions. Amongst these subsegments, the relatively preserved connectivity of limbic-mSN compared to associative-vSN and motor-lSN networks contributes to a growing body of evidence that relative, as opposed to absolute, degeneration amongst SN associated dopaminergic networks determines the impulsivity phenotype. The structural differences identified in this study are associated with susceptibility of PD patients to impulse control behaviors in response to DRT; however, it remains to be elucidated whether these represent a pre-existing biological predisposition or might occur as a result of dopaminergic medications and/or compulsive behaviors modulating the neurobiology of PD. Understanding neural correlates and potential predisposing factors of these severe behavioral symptoms will be crucial to guide clinical practice and to foster preventive strategies in the future.

Funding

This work was partially supported by the Dean's Leadership in Health and Science Scholarship at the David Geffen School of Medicine at UCLA. Additional funding provided by R01NS097882 and U01NS098961. Funding sources had no active role in conducting research.

Declarations of Interest

None.

References

Antonini, A., Barone, P., Bonuccelli, U., Annoni, K., Asgharnejad, M., & Stanzione, P. (2017). ICARUS study: prevalence and clinical features of impulse control disorders in Parkinson's disease. *J Neurol Neurosurg Psychiatry, 88*(4), 317-324. doi:10.1136/jnnp-2016-315277

Behrens, T. E., Berg, H. J., Jbabdi, S., Rushworth, M. F., & Woolrich, M. W. (2007). Probabilistic diffusion tractography with multiple fibre orientations: What can we gain? *Neuroimage, 34*(1), 144-155. doi:10.1016/j.neuroimage.2006.09.018

Besson, M., Pelloux, Y., Dilleen, R., Theobald, D. E., Lyon, A., Belin-Rauscent, A., . . . Belin, D. (2013). Cocaine modulation of frontostriatal expression of Zif268, D2, and 5-HT2c receptors in high and low impulsive rats. *Neuropsychopharmacology, 38*(10), 1963-1973. doi:10.1038/npp.2013.95

Biundo, R., Weis, L., Facchini, S., Formento-Dojot, P., Vallelunga, A., Pilleri, M., . . . Antonini, A. (2015). Patterns of cortical thickness associated with impulse control disorders in Parkinson's disease. *Mov Disord, 30*(5), 688-695. doi:10.1002/mds.26154

Buckholtz, J. W., Treadway, M. T., Cowan, R. L., Woodward, N. D., Li, R., Ansari, M. S., . . . Zald, D. H. (2010). Dopaminergic network differences in human impulsivity. *Science, 329*(5991), 532. doi:10.1126/science.1185778

Cerasa, A., Salsone, M., Nigro, S., Chiriaco, C., Donzuso, G., Bosco, D., . . . Quattrone, A. (2014). Cortical volume and folding abnormalities in Parkinson's disease patients with pathological gambling. *Parkinsonism Relat Disord, 20*(11), 1209-1214. doi:10.1016/j.parkreldis.2014.09.001

Cilia, R., Ko, J. H., Cho, S. S., van Eimeren, T., Marotta, G., Pellecchia, G., . . . Strafella, A. P. (2010). Reduced dopamine transporter density in the ventral striatum of patients with Parkinson's disease and pathological gambling. *Neurobiol Dis, 39*(1), 98-104. doi:10.1016/j.nbd.2010.03.013

Cilia, R., Rossi, C., Frosini, D., Volterrani, D., Siri, C., Pagni, C., . . . Ceravolo, R. (2011). Dopamine Transporter SPECT Imaging in Corticobasal Syndrome. *PLoS ONE, 6*(5), e18301. doi:10.1371/journal.pone.0018301

Claassen, D. O., Stark, A. J., Spears, C. A., Petersen, K. J., van Wouwe, N. C., Kessler, R. M., . . . Donahue, M. J. (2017). Mesocorticolimbic hemodynamic response in Parkinson's disease patients with compulsive behaviors. *Mov Disord, 32*(11), 1574-1583. doi:10.1002/mds.27047

Cools, E., de Pauw, A. S., & Vanderheyden, K. (2011). Cognitive styles in an international perspective: cross-validation of the Cognitive Style Indicator (CoSI). *Psychol Rep, 109*(1), 59-72. doi:10.2466/04.09.11.PR0.109.4.59-72

Dale, A. M., Fischl, B., & Sereno, M. I. (1999). Cortical surface-based analysis. I. Segmentation and surface reconstruction. *Neuroimage, 9*(2), 179-194. doi:10.1006/nimg.1998.0395

Dalley, J. W., Fryer, T. D., Brichard, L., Robinson, E. S., Theobald, D. E., Laane, K., . . . Robbins, T. W. (2007). Nucleus accumbens D2/3 receptors predict trait impulsivity and cocaine reinforcement. *Science, 315*(5816), 1267-1270. doi:10.1126/science.1137073

De Micco, R., Russo, A., Tedeschi, G., & Tessitore, A. (2018). Impulse Control Behaviors in Parkinson's Disease: Drugs or Disease? Contribution From Imaging Studies. *Front Neurol, 9*, 893. doi:10.3389/fneur.2018.00893

Diergaarde, L., Pattij, T., Poortvliet, I., Hogenboom, F., de Vries, W., Schoffelmeer, A. N., & De Vries, T. J. (2008). Impulsive choice and impulsive action predict vulnerability to distinct stages of nicotine seeking in rats. *Biol Psychiatry, 63*(3), 301-308. doi:10.1016/j.biopsych.2007.07.011

Duke, D. C., Moran, L. B., Pearce, R. K., & Graeber, M. B. (2007). The medial and lateral substantia nigra in Parkinson's disease: mRNA profiles associated with higher brain tissue vulnerability. *Neurogenetics, 8*(2), 83-94. doi:10.1007/s10048-006-0077-6

Fan, L., Li, H., Zhuo, J., Zhang, Y., Wang, J., Chen, L., . . . Jiang, T. (2016). The Human Brainnetome Atlas: A New Brain Atlas Based on Connectional Architecture. *Cereb Cortex, 26*(8), 3508-3526. doi:10.1093/cercor/bhw157

Fearnley, J. M., & Lees, A. J. (1991). Ageing and Parkinson's disease: substantia nigra regional selectivity. *Brain, 114 (Pt 5)*, 2283-2301.

Fischl, B., Sereno, M. I., & Dale, A. M. (1999). Cortical surface-based analysis. II: Inflation, flattening, and a surface-based coordinate system. *Neuroimage, 9*(2), 195-207. doi:10.1006/nimg.1998.0396

Frank, M. J., Seeberger, L. C., & O'Reilly R, C. (2004). By carrot or by stick: cognitive reinforcement learning in parkinsonism. *Science, 306*(5703), 1940-1943. doi:10.1126/science.1102941

Gatto, E. M., & Aldinio, V. (2019). Impulse Control Disorders in Parkinson's Disease. A Brief and Comprehensive Review. *Front Neurol, 10*, 351. doi:10.3389/fneur.2019.00351

Goto, Y., & Grace, A. A. (2008). Limbic and cortical information processing in the nucleus accumbens. *Trends Neurosci, 31*(11), 552-558. doi:10.1016/j.tins.2008.08.002

Haber, S. N. (2014). The place of dopamine in the cortico-basal ganglia circuit. *Neuroscience, 282*, 248-257. doi:10.1016/j.neuroscience.2014.10.008

Haber, S. N., & Knutson, B. (2010). The reward circuit: linking primate anatomy and human imaging. *Neuropsychopharmacology, 35*(1), 4-26. doi:10.1038/npp.2009.129

Hammes, J., Theis, H., Giehl, K., Hoenig, M. C., Greuel, A., Tittgemeyer, M., . . . van Eimeren, T. (2019). Dopamine metabolism of the nucleus accumbens and fronto-striatal connectivity modulate impulse control. *Brain, 142*(3), 733-743. doi:10.1093/brain/awz007

Houeto, J. L., Magnard, R., Dalley, J. W., Belin, D., & Carnicella, S. (2016). Trait Impulsivity and Anhedonia: Two Gateways for the Development of Impulse Control Disorders in Parkinson's Disease? *Front Psychiatry, 7*, 91. doi:10.3389/fpsyt.2016.00091

Jenkinson, M., Bannister, P., Brady, M., & Smith, S. (2002). Improved optimization for the robust and accurate linear registration and motion correction of brain images. *Neuroimage, 17*(2), 825-841.

Jimenez-Urbieta, H., Gago, B., de la Riva, P., Delgado-Alvarado, M., Marin, C., & Rodriguez-Oroz, M. C. (2015). Dyskinesias and impulse control disorders in Parkinson's disease: From pathogenesis to potential therapeutic approaches. *Neurosci Biobehav Rev, 56*, 294-314. doi:10.1016/j.neubiorev.2015.07.010

Joutsa, J., Martikainen, K., Niemela, S., Johansson, J., Forsback, S., Rinne, J. O., & Kaasinen, V. (2012). Increased medial orbitofrontal [18F]fluorodopa uptake in Parkinsonian impulse control disorders. *Mov Disord, 27*(6), 778-782. doi:10.1002/mds.24941

Keuken, M. C., & Forstmann, B. U. (2015). A probabilistic atlas of the basal ganglia using 7 T MRI. *Data Brief, 4*, 577-582. doi:10.1016/j.dib.2015.07.028

Loane, C., Wu, K., O'Sullivan, S. S., Lawrence, A. D., Woodhead, Z., Lees, A. J., . . . Politis, M. (2015). Psychogenic and neural visual-cue response in PD dopamine dysregulation syndrome. *Parkinsonism Relat Disord, 21*(11), 1336-1341. doi:10.1016/j.parkreldis.2015.09.042

Majuri, J., & Joutsa, J. (2019). Molecular imaging of impulse control disorders in Parkinson's disease. *Eur J Nucl Med Mol Imaging, 46*(11), 2220-2222. doi:10.1007/s00259-019-04459-5

Maloney, E. M., Djamshidian, A., & O'Sullivan, S. S. (2017). Phenomenology and epidemiology of impulsive-compulsive behaviours in Parkinson's disease, atypical Parkinsonian disorders and non-Parkinsonian populations. *J Neurol Sci, 374*, 47-52. doi:10.1016/j.jns.2016.12.058

Markovic, V., Agosta, F., Canu, E., Inuggi, A., Petrovic, I., Stankovic, I., . . . Filippi, M. (2017). Role of habenula and amygdala dysfunction in Parkinson disease patients with punding. *Neurology, 88*(23), 2207-2215. doi:10.1212/WNL.0000000000004012

Matsumoto, M., & Hikosaka, O. (2009). Two types of dopamine neuron distinctly convey positive and negative motivational signals. *Nature, 459*(7248), 837-841. doi:10.1038/nature08028

O'Sullivan, S. S., Wu, K., Politis, M., Lawrence, A. D., Evans, A. H., Bose, S. K., . . . Piccini, P. (2011). Cue-induced striatal dopamine release in Parkinson's disease-associated impulsive-compulsive behaviours. *Brain, 134*(Pt 4), 969-978. doi:10.1093/brain/awr003

Payer, D. E., Guttman, M., Kish, S. J., Tong, J., Strafella, A., Zack, M., . . . Boileau, I. (2015). [(1)(1)C]-(+)-PHNO PET imaging of dopamine D(2/3) receptors in Parkinson's disease with impulse control disorders. *Mov Disord, 30*(2), 160-166. doi:10.1002/mds.26135

Phu, A. L., Xu, Z., Brakoulias, V., Mahant, N., Fung, V. S., Moore, G. D., . . . Krause, M. (2014). Effect of impulse control disorders on

disability and quality of life in Parkinson's disease patients. *J Clin Neurosci, 21*(1), 63-66. doi:10.1016/j.jocn.2013.02.032

Postuma, R. B., Berg, D., Stern, M., Poewe, W., Olanow, C. W., Oertel, W., . . . Deuschl, G. (2015). MDS clinical diagnostic criteria for Parkinson's disease. *Mov Disord, 30*(12), 1591-1601. doi:10.1002/mds.26424

Premi, E., Pilotto, A., Garibotto, V., Bigni, B., Turrone, R., Alberici, A., . . . Padovani, A. (2016). Impulse control disorder in PD: A lateralized monoaminergic frontostriatal disconnection syndrome? *Parkinsonism Relat Disord, 30*, 62-66. doi:10.1016/j.parkreldis.2016.05.028

Rao, H., Mamikonyan, E., Detre, J. A., Siderowf, A. D., Stern, M. B., Potenza, M. N., & Weintraub, D. (2010). Decreased ventral striatal activity with impulse control disorders in Parkinson's disease. *Mov Disord, 25*(11), 1660-1669. doi:10.1002/mds.23147

Rokosik, S. L., & Napier, T. C. (2012). Pramipexole-induced increased probabilistic discounting: comparison between a rodent model of Parkinson's disease and controls. *Neuropsychopharmacology, 37*(6), 1397-1408. doi:10.1038/npp.2011.325

Ruitenberg, M. F. L., Wu, T., Averbeck, B. B., Chou, K. L., Koppelmans, V., & Seidler, R. D. (2018). Impulsivity in Parkinson's Disease Is Associated With Alterations in Affective and Sensorimotor Striatal Networks. *Front Neurol, 9*, 279. doi:10.3389/fneur.2018.00279

Smith, S. M. (2002). Fast robust automated brain extraction. *Hum Brain Mapp, 17*(3), 143-155. doi:10.1002/hbm.10062

Steeves, T. D., Miyasaki, J., Zurowski, M., Lang, A. E., Pellecchia, G., Van Eimeren, T., . . . Strafella, A. P. (2009). Increased striatal dopamine release in Parkinsonian patients with pathological gambling: a [11C] raclopride PET study. *Brain, 132*(Pt 5), 1376-1385. doi:10.1093/brain/awp054

Tessitore, A., De Micco, R., Giordano, A., di Nardo, F., Caiazzo, G., Siciliano, M., . . . Tedeschi, G. (2017). Intrinsic brain connectivity predicts impulse control disorders in patients with Parkinson's disease. *Mov Disord, 32*(12), 1710-1719. doi:10.1002/mds.27139

Tessitore, A., Santangelo, G., De Micco, R., Vitale, C., Giordano, A., Raimo, S., . . . Tedeschi, G. (2016). Cortical thickness changes in patients with Parkinson's disease and impulse control disorders. *Parkinsonism Relat Disord, 24*, 119-125. doi:10.1016/j.parkreldis.2015.10.013

Tomlinson, C. L., Stowe, R., Patel, S., Rick, C., Gray, R., & Clarke, C. E. (2010). Systematic review of levodopa dose equivalency reporting in Parkinson's disease. *Mov Disord, 25*(15), 2649-2653. doi:10.1002/mds.23429

Tremblay, L., Hollerman, J. R., & Schultz, W. (1998). Modifications of reward expectation-related neuronal activity during learning in primate striatum. *J Neurophysiol, 80*(2), 964-977. doi:10.1152/jn.1998.80.2.964

Tsolaki, E., Downes, A., Speier, W., Elias, W. J., & Pouratian, N. (2018). The potential value of probabilistic tractography-based for MR-guided focused ultrasound thalamotomy for essential tremor. *Neuroimage Clin, 17*, 1019-1027. doi:10.1016/j.nicl.2017.12.018 van Oosten, R. V., Verheij, M. M., & Cools, A. R. (2005). Bilateral nigral 6-hydroxydopamine lesions increase the amount of extracellular dopamine in the nucleus accumbens. *Exp Neurol, 191*(1), 24-32. doi:10.1016/j.expneurol.2004.09.004

Voon, V., Fernagut, P. O., Wickens, J., Baunez, C., Rodriguez, M., Pavon, N., . . . Bezard, E. (2009). Chronic dopaminergic stimulation in Parkinson's disease: from dyskinesias to impulse control disorders. *Lancet Neurol, 8*(12), 1140-1149. doi:10.1016/S1474-4422(09)70287-X

Voon, V., Gao, J., Brezing, C., Symmonds, M., Ekanayake, V., Fernandez, H., . . . Hallett, M. (2011). Dopamine agonists and risk: impulse control disorders in Parkinson's disease. *Brain, 134*(Pt 5), 1438-1446. doi:10.1093/brain/awr080

Voon, V., Napier, T. C., Frank, M. J., Sgambato-Faure, V., Grace, A. A., Rodriguez-Oroz, M., . . . Fernagut, P. O. (2017). Impulse control disorders and levodopa-induced dyskinesias in Parkinson's disease: an update. *Lancet Neurol, 16*(3), 238-250. doi:10.1016/S1474-4422(17)30004-2

Weintraub, D., David, A. S., Evans, A. H., Grant, J. E., & Stacy, M. (2015). Clinical spectrum of impulse control disorders in Parkinson's disease. *Mov Disord, 30*(2), 121-127. doi:10.1002/mds.26016

Weintraub, D., Hoops, S., Shea, J. A., Lyons, K. E., Pahwa, R., Driver-Dunckley, E. D., . . . Voon, V. (2009). Validation of the questionnaire for impulsive-compulsive disorders in Parkinson's disease. *Mov Disord, 24*(10), 1461-1467. doi:10.1002/mds.22571

Weintraub, D., Koester, J., Potenza, M. N., Siderowf, A. D., Stacy, M., Voon, V., . . . Lang, A. E. (2010). Impulse control disorders in Parkinson disease: a cross-sectional study of 3090 patients. *Arch Neurol, 67*(5), 589-595. doi:10.1001/archneurol.2010.65

Wise, R. A. (2009). Roles for nigrostriatal–not just mesocorticolimbic–dopamine in reward and addiction. *Trends Neurosci, 32*(10), 517-524. doi:10.1016/j.tins.2009.06.004

Yoo, H. B., Lee, J. Y., Lee, J. S., Kang, H., Kim, Y. K., Song, I. C., . . . Jeon, B. S. (2015). Whole-brain diffusion-tensor changes in parkinsonian patients with impulse control disorders. *J Clin Neurol, 11*(1), 42-47. doi:10.3988/jcn.2015.11.1.42

Yoo, H. S., Yun, H. J., Chung, S. J., Sunwoo, M. K., Lee, J. M., Sohn, Y. H., & Lee, P. H. (2015). Patterns of Neuropsychological Profile and Cortical Thinning in Parkinson's Disease with Punding. *PLoS One, 10*(7), e0134468. doi:10.1371/journal.pone.0134468

Zhang, Y., Larcher, K. M., Misic, B., & Dagher, A. (2017). Anatomical and functional organization of the human substantia nigra and its connections. *Elife, 6*. doi:10.7554/eLife.26653